Received: 25 December 2023 | Revised: 7 May 2024 | Accepted: 14 May 2024

DOI: 10.1111/cas.16232

ORIGINAL ARTICLE

Cancer Science WILEY

HAS2 facilitates glioma cell malignancy and suppresses ferroptosis in an *FZD7*-dependent manner

Zhiyuan Liu[1] | Kuo Yu[1] | Kaile Chen[1] | Jinlai Liu[1,2] | Kexiang Dai[3] | Peng Zhao[1]

[1]Department of Neurosurgery, The First Affiliated Hospital of Nanjing Medical University, Nanjing, China

[2]Department of Neurosurgery, Yang Zhong, Jiangsu Province People's Hospital, Yangzhou, China

[3]Department of Neurosugery, Emergency General Hospital, Beijing, China

Correspondence
Peng Zhao, Department of Neurosurgery, The First Affiliated Hospital of Nanjing Medical University, No.300 Guangzhou Road, Nanjing 210000, China.
Email: zhaopeng@njmu.edu.cn

Funding information
the Outstanding Young and Middle-aged Talents Support Program of the First Affiliated Hospital with Nanjing Medical University (Jiangsu Province Hospital); Jiangsu Province Capability Improvement Project through Science, Technology and Education, Grant/Award Number: ZDXK202225

Abstract

Glioma is the most common malignant tumor in the central nervous system, and it is crucial to uncover the factors that influence prognosis. In this study, we utilized Mfuzz to identify a gene set that showed a negative correlation with overall survival in patients with glioma. Gene Ontology (GO) enrichment analyses were then undertaken to gain insights into the functional characteristics and pathways associated with these genes. The expression distribution of Hyaluronan Synthase 2 (*HAS2*) was explored across multiple datasets, revealing its expression patterns. In vitro and in vivo experiments were carried out through gene knockdown and overexpression to validate the functionality of *HAS2*. Potential upstream transcription factors of *HAS2* were predicted using transcriptional regulatory databases, and these predictions were experimentally validated using ChIP-PCR and dual-luciferase reporter gene assays. The results showed that elevated expression of *HAS2* in glioma indicates poor prognosis. *HAS2* was found to play a role in activating an antiferroptosis pathway in glioma cells. Inhibiting *HAS2* significantly increased cellular sensitivity to ferroptosis-inducing agents. Finally, we determined that the oncogenic effect of *HAS2* is mediated by the key receptor of the WNT pathway, *FZD7*.

KEYWORDS
ferroptosis resistance, *FZD7*, glioma, *HAS2*, transcriptional regulation

1 | INTRODUCTION

Glioma is a prevalent type of tumor that develops within the central nervous system, specifically originating from the supportive tissues surrounding neurons and neuroglia.[1] This aggressive tumor can manifest in different regions of the brain, such as the cerebral cortex, white matter, and brainstem.[2] Glioma is recognized as one of the most frequent primary brain tumors affecting individuals of all age groups.[3] Glioblastoma multiforme represents the most aggressive and fatal variant of glioma, characterized by its infiltrative growth and the extreme challenge of achieving complete surgical removal.[4] The median survival time for individuals diagnosed with GBM is currently estimated to be approximately 15 months.[5,6]

The tumor microenvironment is a complex milieu consisting of tumor cells, ECM, diverse immune cells, stromal cells, blood vessels, cytokines, growth factors, and distinct physicochemical conditions

Abbreviations: CGGA, Chinese Glioma Genome Atlas; FZD7, Frizzled class receptor 7; GBM, glioblastoma; GO, Gene Ontology; GPX4, glutathione peroxidase 4; GSEA, gene set enrichment analysis; GSH, glutathione; HA, hyaluronic acid; HAS2, hyaluronan synthase 2; HR, hazard ratio; LGG, lower-grade glioma; MDA, malondialdehyde; qPCR, quantitative PCR; ROC, receiver operating characteristic; TCGA, The Cancer Genome Atlas; TEM, transmission electron microscopy; TGF-β, transforming growth factor-β; TP63, tumor protein P63.

Zhiyuan Liu, Kuo Yu, and Kaile Chen contributed equally to this work.

like hypoxia and acidic pH.[7] This intricate environment closely interacts with tumor cells and exerts a substantial influence on their behavior and progression.[8]

The ECM not only serves as a supportive and structural framework but also plays a crucial role in regulating cellular behavior within the glioblastoma microenvironment.[9]

Compared to primary glioblastomas, patients who received standardized treatment showed elevated expression of genes related to the ECM.[10] This change in ECM composition is closely linked to a significant decrease in survival rates among recurrent glioma patients. Additionally, tumor tissue undergoes substantial changes in the composition of ECM components compared to normal tissue.[11,12]

HAS2, being the primary enzyme responsible for synthesizing HA, is frequently found to be highly expressed in glioblastoma tissue.[13] Consequently, this elevated expression results in the excessive accumulation of HA within the tumor microenvironment.[14] The increased levels of HA within glioma tissue have the potential to stimulate the migration, invasion, and proliferation of tumor cells through various signaling pathways.[15] Moreover, HA interacts with other constituents present in the tumor microenvironment, such as tumor-associated cells, vascular endothelial cells, and immune cells. These interactions can modulate the behavior of tumor cells and influence the growth, invasiveness, and response to treatment of glioblastoma.[16,17]

Further research is necessary to fully comprehend the exact mechanisms and functions of *HAS2* in glioblastoma progression. A comprehensive understanding of the association between *HAS2* and glioblastoma is vital for uncovering the molecular mechanisms that drive its development, which can guide the development of innovative therapeutic strategies. In this study, we extensively utilized bioinformatics data and tools to investigate and elucidate the precise mechanisms by which *HAS2* promotes glioblastoma progression. These findings establish a theoretical basis for considering *HAS2* as a potential therapeutic target in future endeavors.

2 | MATERIALS AND METHODS

All methods and materials can be found in Document S1 and Table S1 and S2. In summary, a potential glioblastoma progression-promoting gene, *HAS2*, was identified through Mfuzz, GO enrichment analysis, and survival analysis. This was further supported by in vitro and in vivo experiments including CCK-8 assay, colony formation assay, EdU assay, wound healing assay, Transwell assay, and a xenograft mouse model. Downstream genes and signaling pathways of HAS2 were identified through GSEA. The impact of *HAS2* on ferroptosis in glioblastoma cells was explored through TEM observation and MDA and GSH detection. Potential upstream transcription factors of *HAS2* were predicted using transcriptional regulatory databases and validated by ChIP-PCR and dual-luciferase reporter gene assays. For detailed bioinformatics analysis and experimental procedures, please refer to Document S1.

3 | RESULTS

3.1 | Extracellular matrix-related pathways linked with decreased overall survival among glioma patients

We integrated transcriptomic data from three different cohorts of glioblastoma samples, namely TCGA-GBM, CGGA325, and CGGA693 (Figure 1A). We categorized patients into four subgroups (C1, C2, C3, and C4) based on quartiles of overall survival. To investigate the expression patterns of all genes in these subgroups, we conducted Mfuzz clustering analysis (Figure S1). Notably, genes assigned to clusters 12, 14, and 21 showed consistent upregulation across subgroups C1–C4 (Figure 1B), indicating their potential significance as major drivers of glioblastoma progression.

To gain further insights into the functional implications of these genes, we undertook GO enrichment analyses on the intersection of genes from these clusters and those that were upregulated in glioblastoma (Figure 1C). The enriched GO pathways were external encapsulating structure organization, extracellular structure organization, and ECM organization, indicating that they are primarily associated with pathways related to the ECM (Figure 1D). We further analyzed the fold change and HR values of genes in the top three enriched pathways. The findings reveal that *HAS2* shows higher fold change and HR values (Figure 1E,F).

Hyaluronic acid is a vital component of the ECM and is upregulated in various tumors, impacting cancer cell malignancy. Hyaluronic acid synthesis relies on hyaluronan synthase members (*HAS1*, *HAS2*, and *HAS3*). Interestingly, in glioblastoma, *HAS2* was among the genes identified through Mfuzz clustering analysis and found to be upregulated. This indicates that *HAS2* may play a pivotal role in glioblastoma progression. Additionally, genes assigned to clusters 25, 30, and 45 showed consistent downregulation across subgroups C1 to C4. This suggests that genes within these clusters may act as potential negative regulators of GBM development, contrary to the role of *HAS2* in glioblastoma. We identified 243 genes negatively correlated with *HAS2* expression with $p < 0.05$ from these three clusters using Spearman's correlation coefficient, and the list of these genes is provided in Table S3. Among them, histone deacetylase 11 can directly interact with Twist protein and repress Twist-induced *HAS2* gene transcription, thus inhibiting tumor cell invasion.[18] Histone deacetylase 11 has been repeatedly reported as a negative regulator of GBM progression.[19–22] Tau protein (encoded by the *MAPT* gene) promotes *HAS2* transcription.[23] *MAPT-AS1*, also a member of clusters 25, 30, and 45, negatively correlated with *HAS2* expression, reportedly represses tau translation by competing with rRNA pairing to *MAPT* mRNA internal ribosome entry site (IRES).[24] This suggests that *MAPT-AS1* might also inhibit *HAS2* expression. Additionally, MAPT-AS1 is recognized as a negative regulator of tumor progression.[25,26] These reports also indirectly support the idea that *HAS2* is a key molecule for GBM progression.

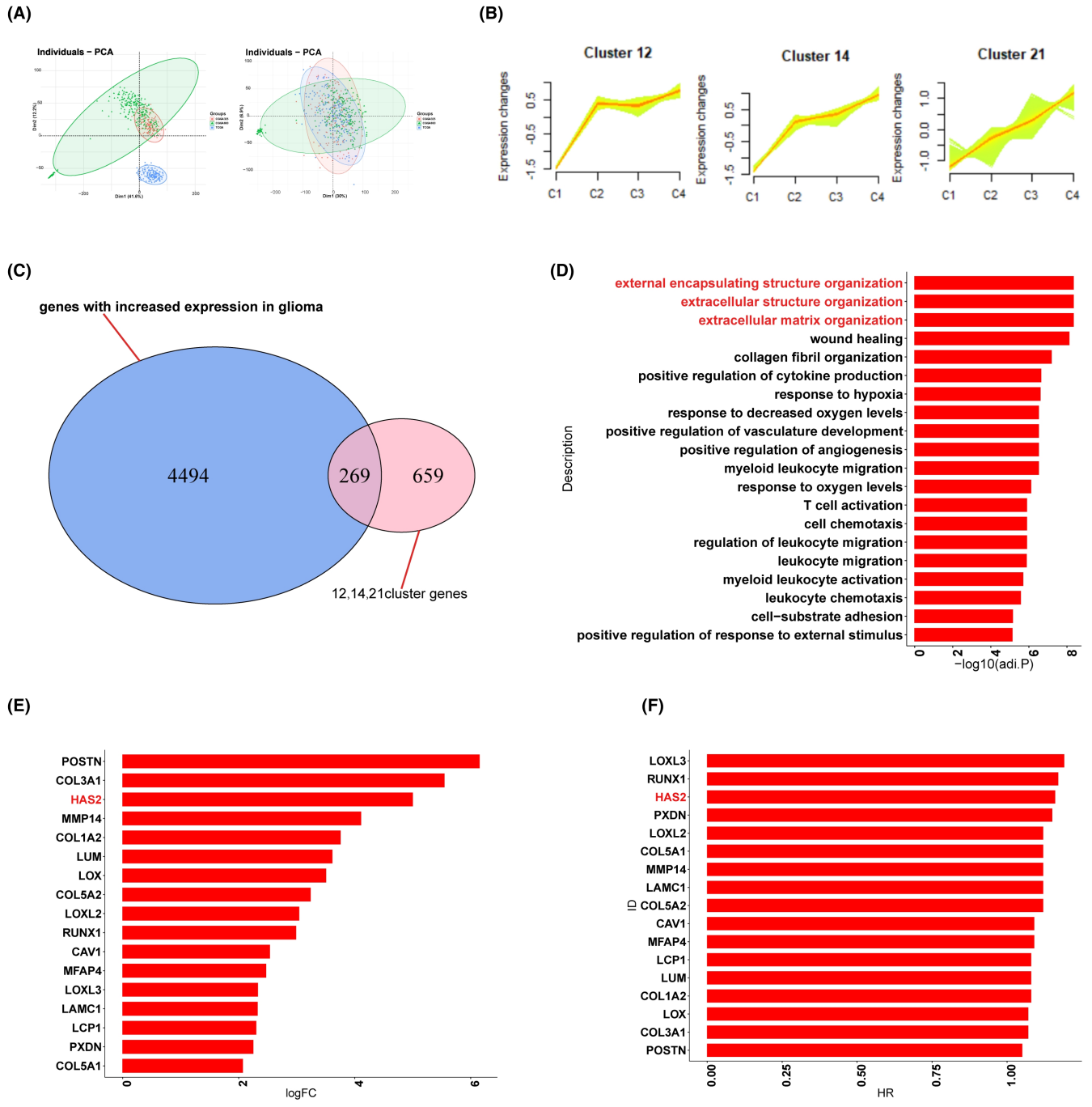

FIGURE 1 Prognostic pathways in patients with glioblastoma (GBM). (A) Principal component analysis (PCA) reveals batch effects in the Chinese Glioma Genome Atlas (CGGA)325, CGGA693, and The Cancer Genome Atlas (TCGA)-GBM cohorts. (B) Mfuzz analysis reveals a consistent upregulation in the expression levels of clusters 12, 14, and 21 across samples C1 to C4. (C) Venn diagram illustrates the overlap between genes that show increased expression in GBM and the genes identified through Mfuzz analysis. (D) Bar plot depicting the Gene Ontology (GO) enrichment analysis results for the intersecting genes. (E, F) Fold change (FC) of specific genes in the GO pathway and the hazard ratio (HR) value.

3.2 | *HAS2* highly expressed in glioma and associated with poor prognosis in patients

Based on the data from CCLE and UALCAN,[27] it has been observed that *HAS2* shows a high expression level in both glioma cell lines and GBM samples (Figure S2A,B). To gain preliminary insights into the potential function of HAS2, we used STRING[28] and GeneMANIA[29] to identify proteins that could have potential interactions with HAS2 (Figure S2D,E).

Through analysis of 10 transcriptome sequencing datasets, we observed significant upregulation of HAS2 in tumor samples compared to normal (Figure 2A). To examine HAS2 expression across glioma grades, considering the correlation between WHO grading and prognosis, we undertook additional investigations. Results showed

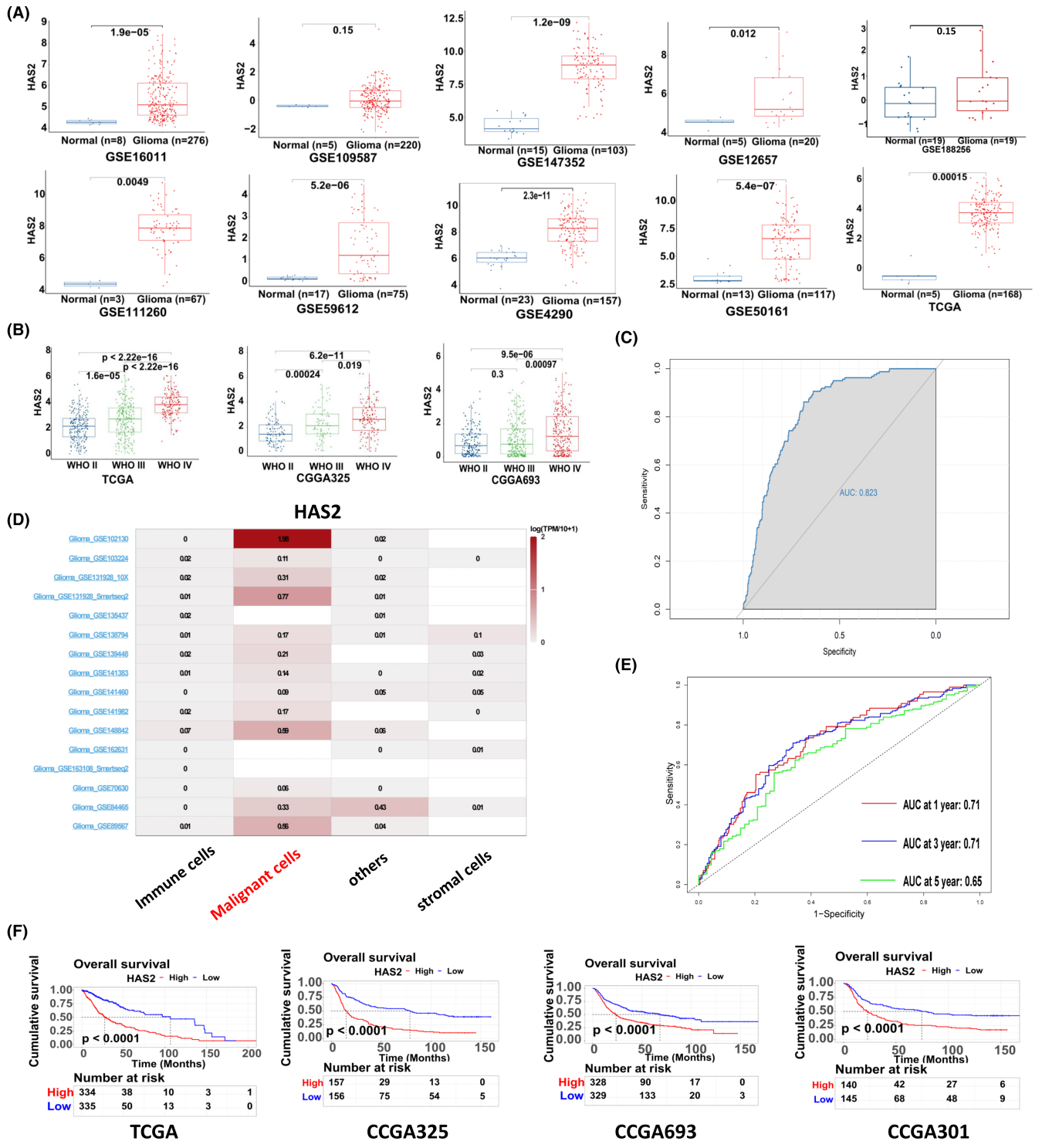

FIGURE 2 Expression level of *HAS2* and its correlation with the clinical characteristics of patients. (A) Expression of *HAS2* in glioma and normal brain cancer tissues. (B) Expression levels of *HAS2* in different grades of glioma. (C) Diagnostic efficacy of *HAS2* in distinguishing between glioblastoma and lower-grade glioma. (D) Single-cell sequencing reveals the expression profile of *HAS2* in different cell types within glioma tissue. (E) Time-dependent receiver operating characteristic curves for 1, 3, and 5-year survival prediction. (F) Kaplan–Meier survival curves for high and low groups based on *HAS2* expression levels. AUC, area under the curve; TCGA, The Cancer Genome Atlas; TPM, transcripts per million.

a positive correlation between HAS2 transcription levels and glioma grades, indicating higher expression as indicative of more aggressive or advanced stages (Figure 2B).

Next, we explored the relationship between *HAS2* and histology, *IDH* mutation status, 1p/19q codeletion status, and age. Results revealed higher HAS2 levels in primary and recurrent GBM, *IDH* WT,

non-codeletion, and age ≥ 42 years (Figure S2C). The ROC curve analysis illustrated that the expression level of *HAS2* could reliably discriminate between GBM and lower-grade glioma (LGG) samples (Figure 2C). Further confirmation was obtained from the single-cell sequencing data of 16 glioma samples collected by TISCH.[30] The analysis revealed that *HAS2* is primarily expressed in glioma cells (Figure 2D).Furthermore, the ROC curves at 1, 3, and 5 years indicated that *HAS2* expression had moderate predictive value for patient prognosis (Figure 2E). The Kaplan–Meier survival curve showed that patients with high expression levels of *HAS2* had a lower median survival time (Figure 2F).

Taken together, these findings indicate that *HAS2* is significantly upregulated in glioma tissues and is closely associated with unfavorable patient prognosis. This suggests that *HAS2* could potentially serve as a valuable prognostic marker for gliomas.

3.3 | *HAS2* silencing inhibits glioma cells proliferation, migration and invasion

The malignant characteristics of glioma cells, such as infiltrative growth and invasiveness, greatly affect treatment effectiveness. Recognizing and addressing these malignancies is crucial for improving treatment outcomes and prognosis in glioma patients.[31]

We used Gene Set Variation Analysis (GSVA) to compute scores for migration, invasion, proliferation, and cell cycle pathways in glioma samples from the TCGA, CGGA325, and CGGA693 datasets. Our results revealed that the high-expression group of *HAS2* shows significantly higher scores in terms of proliferation, migration, and invasion pathways compared to the low-expression group (Figure 3A).

To investigate the role of *HAS2* in glioma progression, we examined the mRNA and protein expression levels of *HAS2* in various glioma cell lines and two human astrocyte cell lines. We observed higher expression of *HAS2* in U87 and LN229 cell lines, while lower expression was found in A172 and U118 cell lines (Figures 3B,C and S5A). To silence *HAS2*, lentiviral particles carrying two shRNAs against HAS2 were individually introduced to U87 and LN229 cells. Following puromycin selection, we established stable transfected glioma cell lines. Quantitative PCR revealed that the two *HAS2* shRNAs effectively silenced over 90% of *HAS2* mRNA compared to the control (shNC) (Figure S3A,B). Consequently, *HAS2* protein levels were significantly downregulated (Figure S4A,B). We undertook a series of in vitro experiments to evaluate whether the silencing of *HAS2* would induce phenotypic changes in glioma cells. The results indicated that *HAS2* silencing led to a marked inhibition of cell viability, clonogenicity, and nuclear EdU incorporation in U87 and LN229 cells (Figures 3D–F and S5B). Furthermore, wound healing assay, Transwell migration assay, and Matrigel Transwell invasion assay showed that *HAS2* silencing significantly inhibited cell migration and invasion (Figures 3G and S5C,D). To further clarify the responsibility of *HAS2*, we carried out the rescue experiment using the shHAS2#1-treated cells ectopically expressed (sh-resistant) WT HAS2. The result confirmed that the ectopic expression of *HAS2* reinstated the malignant characteristics of glioma cells (Figures 3D–G and S5B–D). In addition, we validated the function of *HAS2* in vivo. *HAS2*-silenced U87 (shHAS2#1) cells labeled with luciferase and relevant control cells were injected into the frontal subdural region of nude mice. The nude mice with *HAS2*-silenced cells showed weaker bioluminescent intensity and longer survival time compared to the control group (Figure 3H–J). In conclusion, our findings suggest that HAS2 silencing inhibits proliferation, migration, and invasion of glioma cells.

3.4 | Overexpression of *HAS2* promotes glioma cells proliferation, migration, and invasion

To further investigate the function of *HAS2* in glioma cells, *HAS2*-WT expression vector, *HAS2*-K190R mutant (catalytically inactive *HAS2*)[32] expression vector, or empty vector was stably transfected into cells with low *HAS2* expression (A172 and U118). Overexpression of *HAS2* was confirmed by qPCR and western blot experiments (Figures S3C,D and S4C,D). Overexpression of *HAS2*-WT significantly enhanced cell viability (Figure 4A), clonogenicity (Figure 4B), and nuclear EdU incorporation (Figure 4C) in A172 and U118 cells. However, *HAS2*-K190R did not have such an effect. Additionally, both wound healing and Transwell migration assays showed that ectopic expression of *HAS2*-WT augmented the migratory ability of glioma cells (Figure 4D,E). The Matrigel Transwell invasion assay also revealed that *HAS2*-WT overexpression promoted glioma cell invasion (Figure 4E). Similarly, catalytically inactive *HAS2* did not significantly alter the migration or invasion abilities of glioma cells. Furthermore, nude mice injected with *HAS2*-WT overexpression U118 cells displayed increased bioluminescence signals and shorter survival time compared with the relevant control (Figure 4F–H). These findings provide evidence that overexpression of *HAS2* promotes proliferation, invasion, and migration of glioma cells in an enzyme activity-dependent manner.

3.5 | *HAS2* inhibits ferroptosis in glioma cells

To investigate the role of *HAS2* in glioma cells, we undertook differential and GSEA enrichment analyses using median grouping based on *HAS2* expression levels. Our findings revealed a correlation between *HAS2* and activation of the ferroptosis inhibition pathway (Figure 5A). High expression of *HAS2* in glioma cells could confer resistance to ferroptosis, highlighting its importance in cancer cell behavior.

Even though glioma cells frequently experience oxidative stress and show increased iron uptake, they demonstrate a remarkable resistance to a form of cell death called ferroptosis.[33] Overcoming the resistance of cancer cells, including glioma cells, to ferroptosis has emerged as a significant objective in cancer therapy.

To induce ferroptosis, we treated U87 and LN229 cell lines with erastin, a compound known for its ability to trigger this specific form of cell death. Using TEM, we observed typical ferroptotic

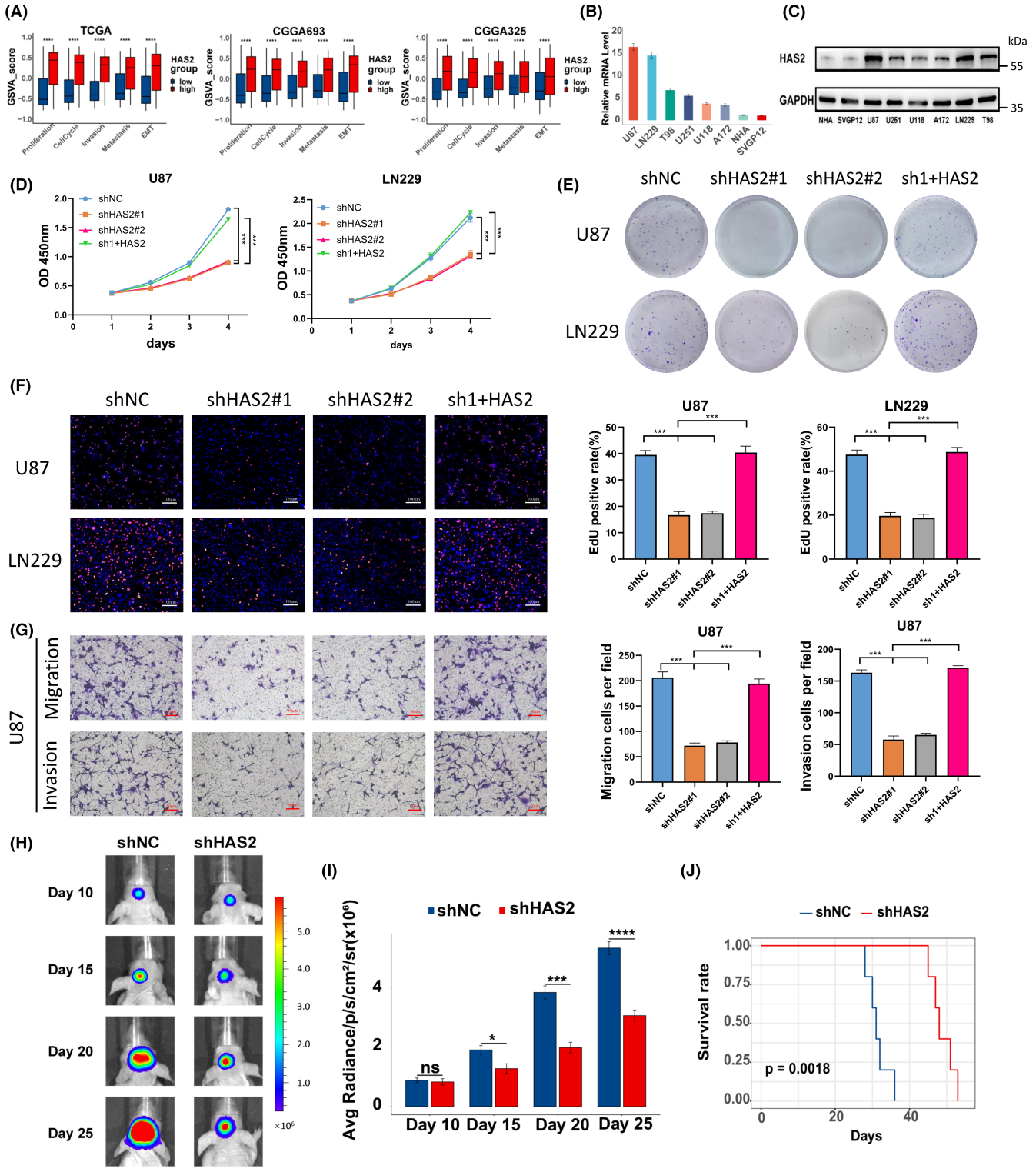

FIGURE 3 Association between *HAS2* and malignant phenotypes of glioma. (A) Box plots illustrating the relationship between *HAS2* expression levels and proliferation, cell cycle, migration, and invasion scores. (B, C) Expression levels of *HAS2* in different cell lines. (D) CCK-8 assay revealed the proliferative activity of glioma cells under different *HAS2* treatments. (E) Representative images of colony formation assay following *HAS2* knockdown and rescue. (F) EdU assay showed changes in glioma proliferation capacity following *HAS2* knockdown and rescue. (G) Representative images and quantitative analysis of Transwell migration and invasion assays in U87 cells following *HAS2* treatment. (H, I) Representative images of the orthotopic xenograft model and quantitative analysis of fluorescence intensity. (J) Difference in survival time between two groups of mice. All experiments were independently repeated at least three times. Student's *t*-test was used for comparisons between two groups, one-way ANOVA followed by Tukey's post hoc test was used for comparisons among three or more groups. $^{*}p<0.05$, $^{**}p<0.01$, $^{***}p<0.001$, $^{****}p<0.0001$. CCGA, Chinese Glioma Genome Atlas; OD, optical density; ns, no significance; shNC, control; TCGA, The Cancer Genome Atlas.

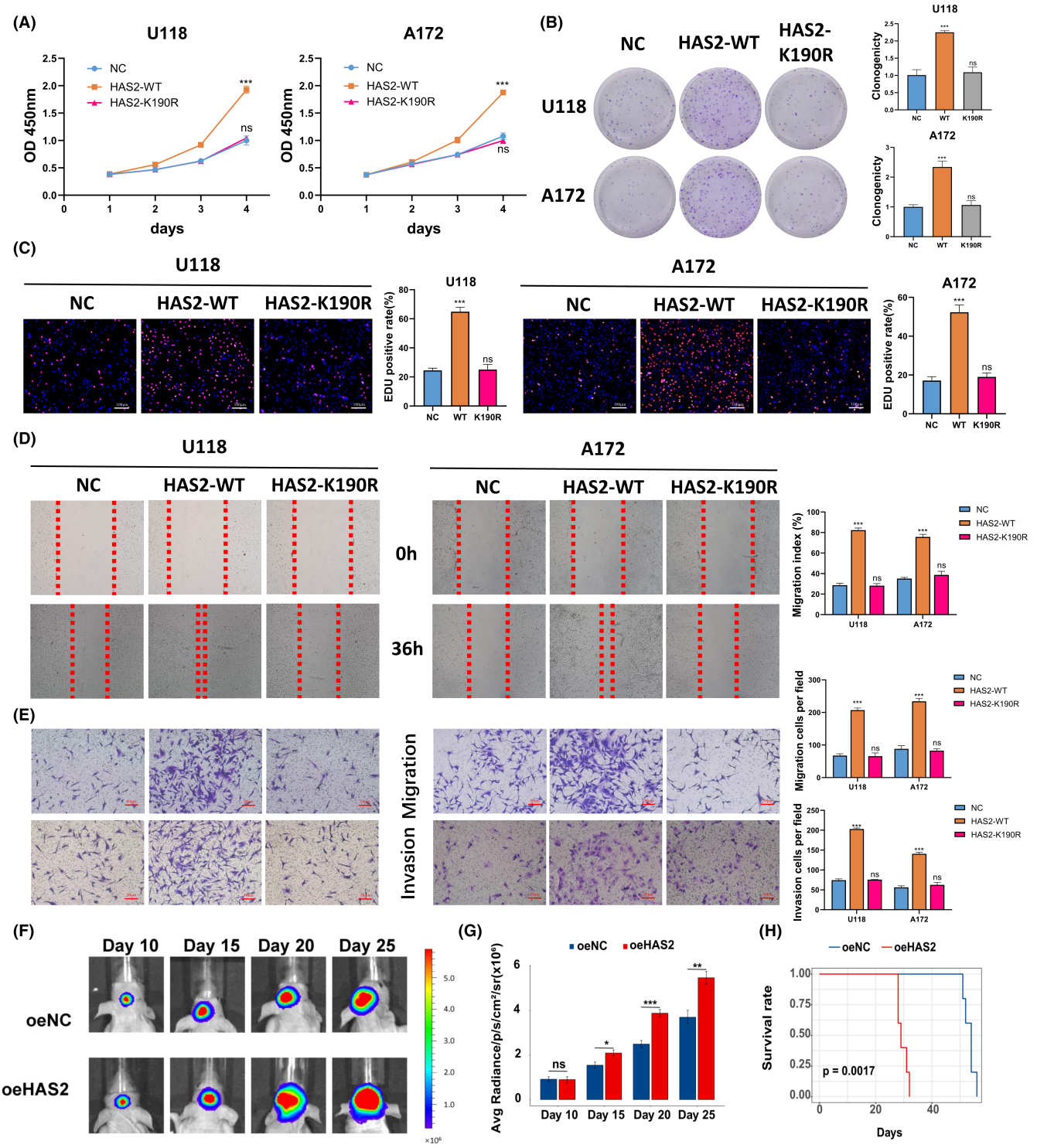

FIGURE 4 Effects of *HAS2* overexpression (oe) on glioma cells. (A) Cell viability of glioma cells overexpressing WT *HAS2* and *HAS2*-K190R were detected by CCK-8 assay. (B) Representative images and quantitative analysis of colony formation assays. (C) EdU assay confirmed that *HAS2*-WT, but not *HAS2*-K190R, enhances proliferation capacity of glioma cells. (D) Representative images and quantitative analysis of scratch assays in cells overexpressing *HAS2*-WT or *HAS2*-K190R. (E) Transwell assay confirmed that overexpression of WT *HAS2* promotes migration and invasion of glioma cells. (F, G) Representative images of the orthotopic xenograft model and quantitative analysis of fluorescence intensity. (H) Overexpression of *HAS2* (WT) in glioma cells leads to shorter survival in mice. All experiments were independently repeated at least three times. Student's *t*-test was used for comparisons between two groups, one-way ANOVA followed by Tukey's post hoc test was used for comparisons among three or more groups. $^{*}p<0.05$, $^{**}p<0.01$, $^{***}p<0.001$, $^{****}p<0.0001$. NC, control; ns, not significant; OD, optical density.

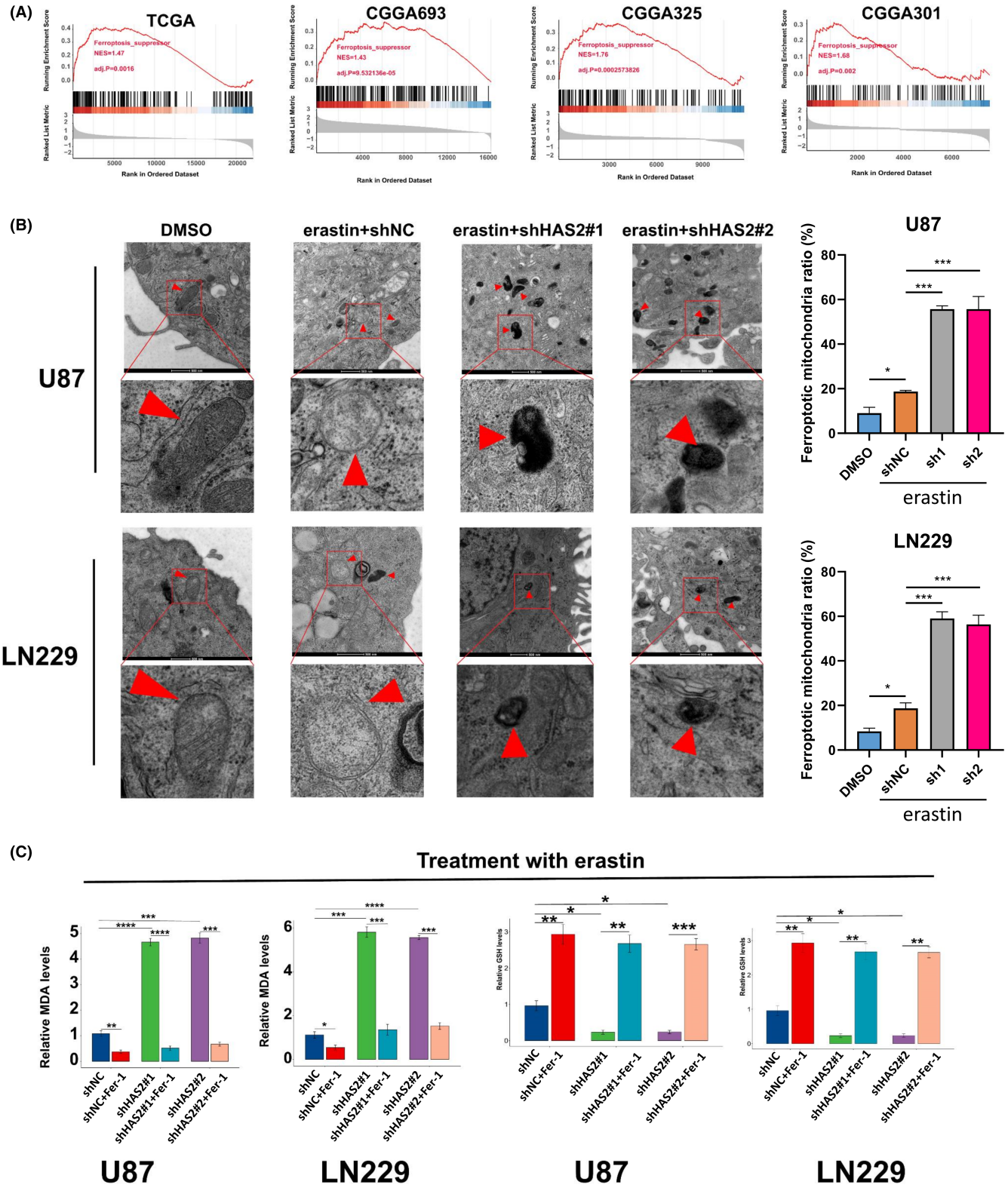

FIGURE 5 *HAS2* inhibits ferroptosis in glioma cells. (A) Gene set enrichment analysis indicated a significant positive correlation between the activation of *HAS2* and the ferroptosis suppressor pathway. (B) Transmission electron microscopy images of mitochondrial morphology under different treatment conditions. (C) Relative levels of malondialdehyde (MDA) and glutathione (GSH) in *HAS2* knockdown and control groups under erastin treatment. All experiments were independently repeated at least three times. Student's *t*-test was used for comparisons between two groups, one-way ANOVA followed by Tukey's post hoc test was used for comparisons among three or more groups. $^{*}p<0.05$, $^{**}p<0.01$, $^{***}p<0.001$; $^{****}p<0.0001$. CCGA, Chinese Glioma Genome Atlas; NES, normalized enrichment score; shNC, control; TCGA, The Cancer Genome Atlas.

characteristics, including shrunken mitochondria, shrinking or disappearing mitochondrial cristae, and increased mitochondrial membrane density in the shHAS2 group (Figure 5B). In line with this, downregulating *HAS2* expression in glioma cells resulted in increased levels of lipid peroxidation, a hallmark of ferroptosis, and decreased content of GSH (Figure 5C). Additionally, ferrostatin-1, the ferroptosis inhibitors can counteract the increased MDA levels and decreased GSH levels caused by the inhibition of *HAS2* (Figure 5C). In conclusion, the high expression of *HAS2* in glioma cells is closely associated with its resistance to ferroptosis.

3.6 | *HAS2* promotes ferroptosis resistance in glioma cells through *FZD7/β-catenin*

To further elucidate the mechanism of *HAS2* inhibition on ferroptosis, we assessed the correlation between *HAS2* expression levels and the activity of various pathways using progeny analysis.[34] The results (Figure 6A) revealed that *HAS2* showed the highest correlation and most significant *p* value with the WNT pathway. Western blot analysis validates that the protein expression of both total *β-catenin* and nuclear *β-catenin* significantly decreases following *HAS2* knockdown (Figures 6B and S6C). The combination of LF3 (a specific inhibitor of Wnt/β-catenin) and erastin significantly increased MDA levels and decreased GSH levels, while ferrostatin-1 was able to inhibit this effect (Figures 6C and S6A,B). This suggests that the Wnt pathway plays a role in resisting ferroptosis in glioma cells. Furthermore, SKL2001 (a Wnt/β-catenin agonist) was able to reverse the ferroptotic effect caused by *HAS2* knockdown (Figure 6D,E). This suggests that the antiferroptotic effect of *HAS2* is mediated by the Wnt signaling pathway. Previous research suggests that the activated WNT pathway targets the transcription of *GPX4* to inhibit ferroptosis.[35]

FZD7, a key receptor in the WNT pathway, has been found to play a crucial role in inhibiting ferroptosis. It accomplishes this by promoting the activation of *β-catenin*, facilitating its translocation into the nucleus, and subsequently enhancing the transcription of *TP63*.[36] *TP63* possesses the ability to inhibit cell damage induced by oxidative stress through a specific mechanism. It exerts its effect by promoting the transcription of *GPX4*, which subsequently enhances the synthesis of glutathione.[37] The heatmap analysis of 14 datasets indicated a positive correlation between the expression levels of *HAS2* and *FZD7* (Figure 6F). *HAS2* knockdown leads to decreased *FZD7* expression, whereas *HAS2* overexpression results in increased *FZD7* expression (Figure 6G). The overexpression of *FZD7* can restore the expression level of *β-catenin* when *HAS2* is knocked down (Figure 6H and S6D). This indicates that *HAS2* indeed affects the activity of the WNT pathway by promoting the expression of *FZD7*. Finally, the expression changes of *FZD7* and *β-catenin* show consistency with the alterations observed in *HAS2* (Figure 6I,J and S6E,F).

In a word, the increased *HAS2* expression in glioma cells confers notable resistance to ferroptosis. This resistance is mediated by the upregulation of *FZD7* expression, facilitated by *HAS2*.

3.7 | *FZD7* mediates the oncogenic effects of *HAS2*

Although we have confirmed that *HAS2* regulates the expression of *FZD7*, it is still unclear whether the former's oncogenic effects are mediated through the latter. Single-cell data suggests that *FZD7* and *HAS2* expression have similar distribution patterns (Figure S7A). The transcription and protein levels of *FZD7* are higher in glioma compared to normal brain tissue, and the expression of *FZD7* is associated with poor prognosis in patients (Figures 7A and S7B). The immunohistochemistry images from HPA[38] also indicate that the expression of *FZD7* is higher in GBM patients compared to LGG patients and normal individuals (Figure S7C).

Transmission electron microscopy revealed that elevated *FZD7* partially reverses the mitochondrial shrinkage and increased membrane density caused by *HAS2* inhibition-induced ferroptosis (Figure 7B). Furthermore, overexpression of *FZD7* in cells with inhibited *HAS2* resulted in a decrease in MDA levels and an increase in GSH levels (Figure 7C,D). The CCK-8, colony formation, and EdU assays showed that overexpression of *FZD7* can restore the proliferation inhibition caused by *HAS2* knockdown in glioma cells (Figure 7E–G). Transwell assays indicated that the migration and invasion abilities of the *HAS2* knockdown/*FZD7* overexpression group are higher compared to the *HAS2* knockdown group (Figure 7H).

The above results strongly suggest that *FZD7* plays a crucial role in mediating the oncogenic effects of *HAS2*.

3.8 | Identification of upstream transcription factors of *HAS2*

Considering the significant impact of *HAS2* on glioma cells, it is imperative to identify the upstream transcription factors that govern its regulation.

We predicted potential transcription factors of *HAS2* using four different types of transcription factor prediction databases: JASPAR,[39] Cistrome DB,[40] KnockTF,[41] and GTRD.[42] SNAI2 was selected for experimental validation as it was found to be a common intersection among these databases (Figure 8A). We analyzed the expression correlation between *SNAI2* and *HAS2* in 33 cancer tissues from TCGA. Positive expression correlation was observed between *SNAI2* and *HAS2* in various tumor types (Figure 8B). Immunofluorescence images from HPA[38] showed nuclear localization of *SNAI2* in glioma cells (Figure 8C), indicating its potential role as a transcription factor. Inhibition of *SNAI2* led to decreased expression of *HAS2*, while overexpression of *SNAI2* resulted in its upregulation (Figures 8D and S8A). Furthermore, the luciferase reporter assay confirmed that *SNAI2* enhances the transcriptional activity of *HAS2* (Figure 8E). Using JASPAR, we predicted potential binding sites where *SNAI2* interacts with the promoter region of *HAS2* (Figure 8F), providing insight into the regulatory mechanism of *SNAI2* on *HAS2* expression. The ChIP-qPCR analysis revealed a strong association between *SNAI2* and site 3, demonstrating its binding capability (Figure 8G). We verified this binding in *SNAI2* knockdown and overexpression cell lines through ChIP-qPCR (Figure 8H).

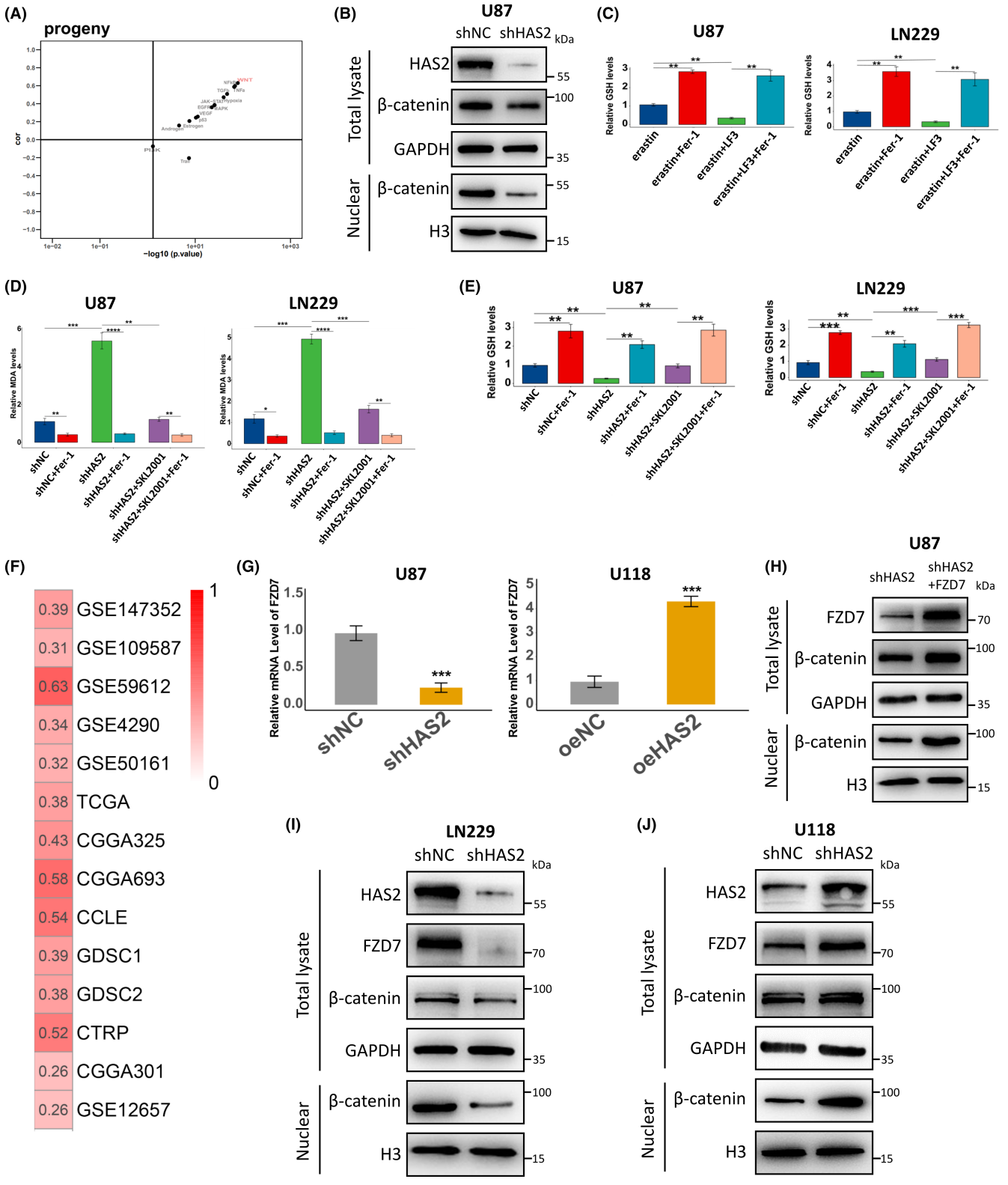

FIGURE 6 *HAS2* promotes ferroptosis resistance in glioma cells through *FZD7*/*β-catenin*. (A) Correlation and *p* values of the activity of 14 pathways in progeny with respect to *HAS2*. (B) Alteration in the activity of the WNT/β-catenin pathway following knockdown of *HAS2*. (C) Relative changes of glutathione (GSH) levels following combined treatment of WNT inhibitor and erastin. (D, E) Relative levels of malondialdehyde (MDA) and GSH in three groups, shNC (control), shHAS2, and shHAS2 combined with SKL2001. (F) Correlation between the expression of *HAS2* and *FZD7* in various public datasets. (G) Relative mRNA levels of *FZD7* after *HAS2* knockdown and overexpression. (H) Expression levels of *β-catenin* in two groups: shHAS2 and shHAS2 + FZD7. (I, J) Changes in protein levels of *FZD7* and *β-catenin* following *HAS2* knockdown and overexpression. All experiments were independently repeated at least three times. Student's *t*-test was used for comparisons between two groups, one-way ANOVA followed by Tukey's post hoc test was used for comparisons among three or more groups. $^{**}p < 0.01$, $^{***}p < 0.001$, $^{****}p < 0.0001$.

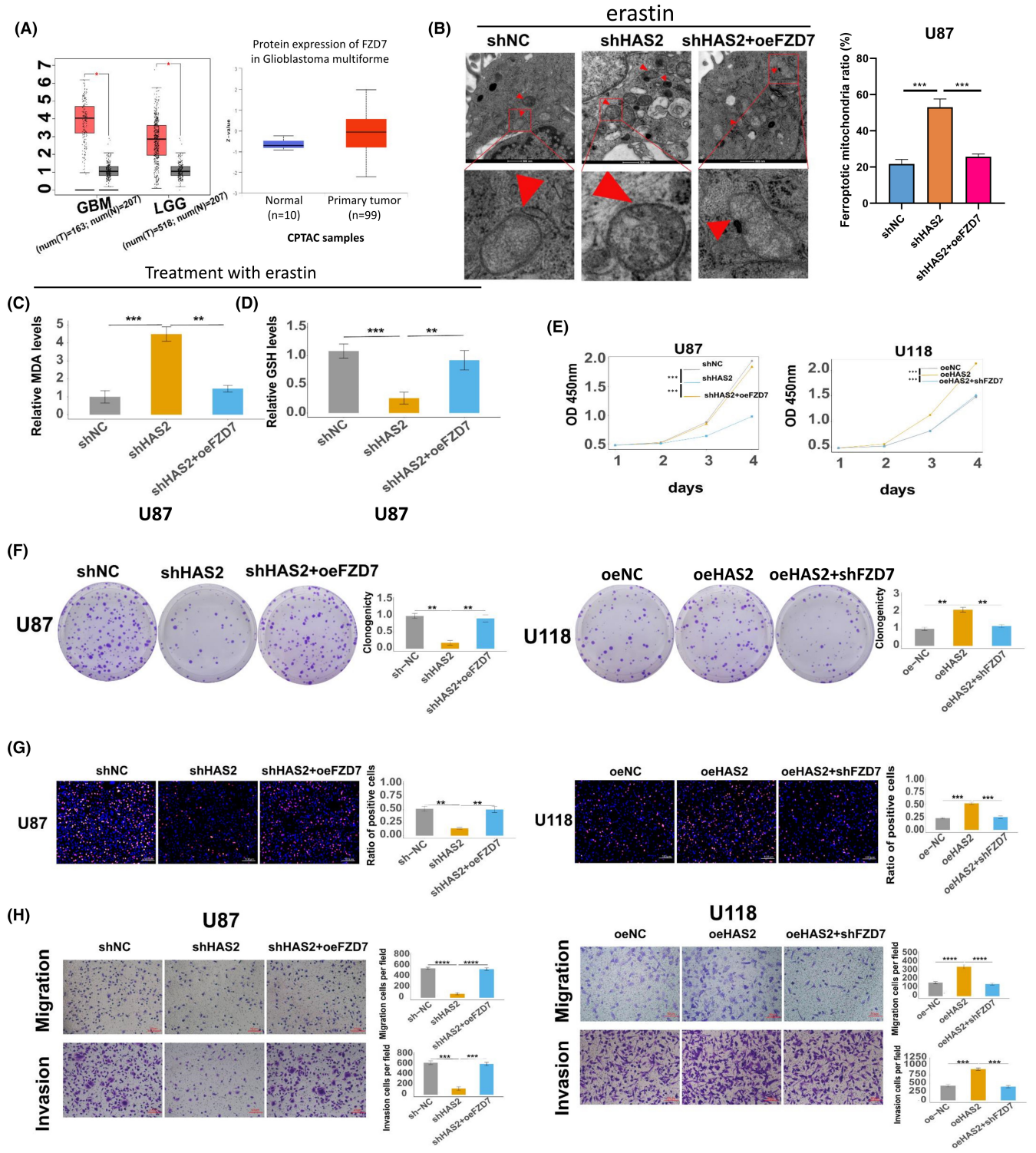

FIGURE 7 *FZD7* plays a crucial role in mediating the function of *HAS2*. (A) Expression levels of *FZD7* in glioblastoma (GBM) (T) and normal (N) tissues. (B) Representative transmission electron microscopy images and quantitative analysis under different treatments. (C, D) Relative levels of malondialdehyde (MDA) and glutathione (GSH) in control group, shHAS2 group, and rescue group. (E–G) Role of *FZD7* in the oncogenic effect of *HAS2* was substantiated through CCK-8, colony formation, and EdU assays. (H) *FZD7* could restore the effects of *HAS2* changes on cell migration and invasive capacity. All experiments were independently repeated at least three times. Student's *t*-test was used for comparisons between two groups, one-way ANOVA followed by Tukey's post hoc test was used for comparisons among three or more groups. $^{**}p<0.01$, $^{***}p<0.001$, $^{****}p<0.0001$. CPTAC, Clinical Proteomic Tumor Analysis Consortium; LGG, lower-grade glioma; OD, optical density; oe, overexpression.

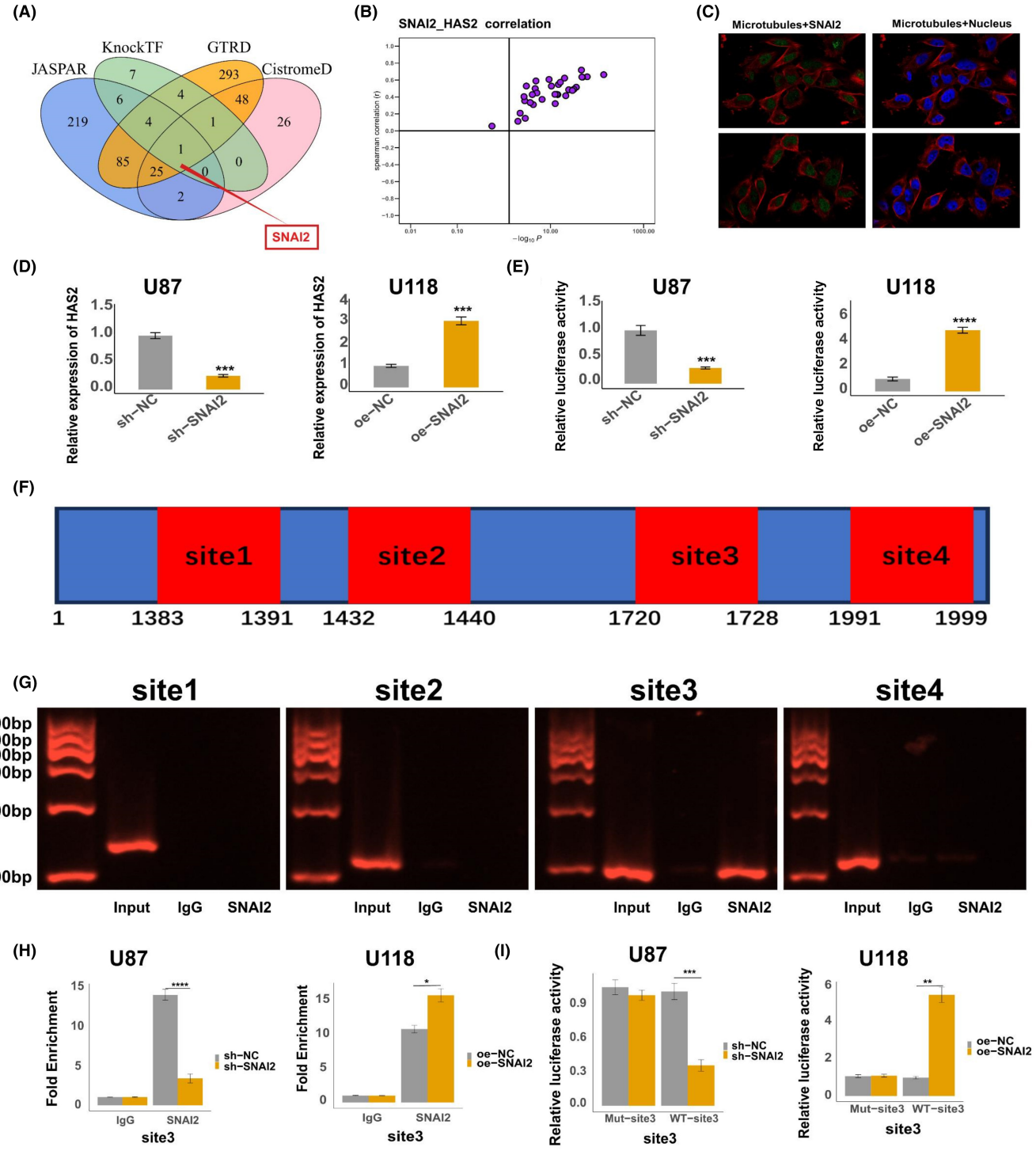

FIGURE 8 *SNAI2* directly binds to the *HAS2* promoter to promote increased expression. (A) Venn diagram visually illustrates the overlap among different databases in their predictions of transcription factors for *HAS2*. (B) Correlation between *SNAI2* and *HAS2* expression in 33 different cancer tissues from The Cancer Genome Atlas. (C) Subcellular localization of *SNAI2*. (D) Expression levels of *HAS2* mRNA changed concordantly with alterations in *HAS2* expression. (E) Dual-luciferase reporter gene assays confirmed *SNAI2* enhanced the transcriptional activity of *HAS2*. (F) Schematic diagram of promoter binding sites. (G) Agarose gel electrophoresis confirmed significant binding of *SNAI2* to binding site 3. (H) ChIP-quantitative PCR further confirmed this binding in *SNAI2* knockdown and overexpression (oe) cell lines. (I) Mutations (Mut) in the sequence of binding site 3 eliminated the changes in luciferase intensity caused by *SNAI2* overexpression or knockdown. All experiments were independently repeated at least three times. Student's *t*-test was used for comparisons between two groups, one-way ANOVA followed by Tukey's post hoc test was used for comparisons among three or more groups. $^{***}p<0.001$, $^{****}p<0.0001$. NC, control.

Moreover, when site 3 was mutated, *SNAI2* no longer exerted its regulatory influence on *HAS2* expression, suggesting the critical role of this specific binding site in mediating *SNAI2*'s impact on *HAS2* transcription (Figure 8I). Subsequently, we further investigated the role of *SNAI2* for transduction of the *HAS2-FZD7*-ferroptosis signaling pathway. Through fractionation–western blot analysis following *SNAI2* knockdown and overexpression in glioma cell lines, we observed a decrease in *FZD7* expression levels following *SNAI2* downregulation, accompanied by a concurrent reduction in Wnt/β-catenin signaling activity (Figure S8A). Conversely, *SNAI2* overexpression yielded the opposite effect (Figure S8A). Additionally, we evaluated the impact of *SNAI2* modulation on the occurrence of ferroptosis in glioma cells. Downregulating *SNAI2* expression in glioma cells resulted in increased levels of MDA and decreased content of GSH (Figure S8B), and ferrostatin-1 could counteract the increased MDA levels and decreased GSH levels. Similarly, overexpression of *SNAI2* was found to decrease MDA levels and elevate GSH levels in U118 cells, while the use of ferroptosis inhibitors did not seem to significantly enhance this trend (Figure S8C). Under TEM observation, *SNAI2* knockdown cells showed marked ferroptotic features, whereas cells overexpressing *SNAI2* showed resistance to erastin-induced ferroptosis (Figure S8D). In conclusion, our study provides compelling evidence that *SNAI2* exerts its role as a positive transcription factor for *HAS2* in glioblastoma cells.

4 | DISCUSSION

Glioblastoma patients often experience recurrence after initial treatment, leading to poor prognosis and limited survival rates. Emerging evidence suggests that remodeling of ECM plays a crucial role in the development of chemoradioresistance and the recurrence of GBM.[10] The ECM is a complex network of proteins, glycoproteins, and proteoglycans surrounding cells within the tumor microenvironment.[43] It provides structural support, regulates cell behaviors, and influences interactions between cells and their surroundings. In healthy tissue, the ECM maintains tissue homeostasis through dynamic remodeling processes involving synthesis, degradation, and modification of its components. However, in GBM, aberrant ECM remodeling occurs, contributing to disease progression and treatment resistance.[44]

Consistent with previous knowledge, our analyses provide additional evidence supporting the association between ECM-related pathways and poor prognosis in GBM. *HAS2*, as one of the key genes in the ECM pathway, is known to be associated with aggressive behaviors in various tumors.[45] Using UALCAN, we present the expression levels of *HAS2* in tumor and normal tissues.

To further elucidate the mechanisms by which *HAS2* promotes aggressive behaviors in GBM, we analyzed *HAS2* in multiple glioma datasets and found that it is associated with the activation of ferroptosis inhibition pathways. This finding was further validated through experimental results.

Ferroptosis is a unique mode of regulated cell death characterized by iron-dependent lipid peroxidation.[46] The ability of glioma cells to evade this particular cell death pathway highlights their adaptability and robust survival mechanisms, further complicating the development of effective therapeutic strategies against gliomas.

Additionally, we confirmed that *HAS2* promotes the expression of *FZD7*, which subsequently leads to the upregulation of *GPX4*. We determined the differential expression of *FZD7* between cancerous and corresponding normal tissues (Figure S7D). *GPX4* inhibits ferroptosis by suppressing lipid peroxidation.[47] Multiple datasets also show a positive correlation between the expression of *HAS2* and *FZD7*. This finding indicates that genes related to the ECM do have the potential to regulate intracellular metabolic states. However, the specific mechanism through which *HAS2* regulates the expression of *FZD7* is still unknown. Further research is needed to elucidate this molecular mechanism and understand the role of *HAS2* in regulating *FZD7* expression. There are reports suggesting that *HAS2* can synthesize HA to activate cell surface receptors, thereby regulating downstream genes or signaling pathways. Binding of HA to the cell surface receptor *CD44* can activate the Nanog homeobox protein (*Nanog*) and promote its nuclear translocation, thereby facilitating the transcription of stem cell regulators *Rex1* and *Sox2*.[48] Additionally, HA binding to *CD44* can activate the PI3K/Akt signaling pathway, thereby promoting the transcriptional expression of *MMP-2* and *MMP-9*, facilitating tumor invasion.[49] In addition to *CD44*, HA synthesized by *HAS2* has been reported to bind to other receptor proteins such as receptor for hyaluronan-mediated motility (RHAMM), Toll-like receptors 2 and 4 (TLR-2 and -4), and lymphatic vessel hyaluronan receptor (LYVE), exerting regulatory effects on genes or signaling pathways.[50,51] These mechanisms depends on the enzymatic activity of HAS, which is consistent with what we observed in Figure 4. Interestingly, Porsch et al. reported that TGF-β-induced *HAS2* expression can promote the mRNA transcription of EMT markers fibronectin, *Snail1*, or *Zeb1*. This effect is independent of both HA and *CD44*. Further studies with *HAS2*-K190R revealed that the role of *HAS2* in TGF-β-mediated EMT is independent of its hyaluronan synthesizing activity.[52] This suggests that the regulatory mechanisms of *HAS2* on downstream genes or signaling pathways are complex and diverse.

Through comprehensive analysis using four transcription factor prediction databases, which consider different aspects, combined with experimental validation, we have successfully identified *SNAI2* as an upstream transcription factor of *HAS2*. *SNAI2*, a well-known transcription factor that promotes EMT transformation in cancer cells, facilitates the proliferation and invasion of GBM.[53] Furthermore, studies have indicated that *SNAI2* plays a role in inhibiting ferroptosis in ovarian cancer.[54]

In summary, our combined approach of bioinformatics analysis and experimental validation has revealed that *HAS2* is an important target in glioblastoma resistance to ferroptosis. The high expression of *HAS2* in gliomas is, to some extent, influenced by increased levels of *SNAI2*. Moreover, we have discovered that the activation of the ferroptosis inhibition pathway by *HAS2* is achieved through the downstream molecule *FZD7*.

AUTHOR CONTRIBUTIONS

Zhiyuan Liu: Conceptualization; investigation; methodology; validation; visualization; writing – original draft; writing – review and

editing. **Kuo Yu:** Conceptualization; formal analysis; investigation; software; validation; visualization; writing – original draft; writing – review and editing. **Kaile Chen:** Data curation; formal analysis; investigation. **Jinlai Liu:** Methodology; software; supervision. **Kexiang Dai:** Data curation; investigation; validation. **Peng Zhao:** Conceptualization; funding acquisition; project administration; resources; supervision; writing – review and editing.

ACKNOWLEDGMENTS

The authors have nothing to report.

FUNDING INFORMATION

This study was funded by the Outstanding Young and Middle-aged Talents Support Program of the First Affiliated Hospital with Nanjing Medical University (Jiangsu Province Hospital), Jiangsu Province Capability Improvement Project through Science, Technology and Education (ZDXK202225).

CONFLICT OF INTEREST STATEMENT

The authors have no conflict of interest.

DATA AVAILABILITY STATEMENT

The data that support the findings of this study are available from the corresponding author upon reasonable request.

ETHICS STATEMENTS

Approval of the research protocol by an institutional review board: The authors declare that the study was approved and conducted in accordance with the policies of the Scientific Ethics Committee of the Nanjing Medical University.

Informed consent: N/A.

Registry and the registration no. of the study/trial: N/A.

Animal studies: All animal protocols were approved by the Animal Management Rule of the Chinese Ministry of Health and the Nanjing Medical University Animal Experimental Ethics Committee.

ORCID

Zhiyuan Liu https://orcid.org/0009-0006-9768-9685

Peng Zhao https://orcid.org/0000-0002-6532-9830

REFERENCES

1. Kondo T. Glioblastoma-initiating cell heterogeneity generated by the cell-of-origin, genetic/epigenetic mutation and microenvironment. *Semin Cancer Biol*. 2022;82:176-183. doi:10.1016/j.semcancer.2020.12.003
2. Ostrom QT, Gittleman H, Liao P, et al. CBTRUS statistical report: primary brain and central nervous system tumors diagnosed in the United States in 2007-2011. *Neuro Oncol*. 2014;16 Suppl 4(Suppl 4):iv1-63:iv1-i63. doi:10.1093/neuonc/nou223
3. Stupp R, Brada M, van den Bent MJ, Tonn JC, Pentheroudakis G, ESMO Guidelines Working Group. High-grade glioma: ESMO clinical practice guidelines for diagnosis, treatment and follow-up. *Ann Oncol*. 2014;25 Suppl 3:iii93-iii101. doi:10.1093/annonc/mdu050
4. Oraiopoulou ME, Tzamali E, Papamatheakis J, Sakkalis V. Phenocopying glioblastoma: a review. *IEEE Rev Biomed Eng*. 2023;16:456-471. doi:10.1109/RBME.2021.3111744
5. Schaff LR, Mellinghoff IK. Glioblastoma and other primary brain malignancies in adults: a review. *JAMA*. 2023;329(7):574-587. doi:10.1001/jama.2023.0023
6. Louis DN, Perry A, Wesseling P, et al. The 2021 WHO classification of tumors of the central nervous system: a summary. *Neuro Oncol*. 2021;23(8):1231-1251. doi:10.1093/neuonc/noab106
7. Goliwas KF, Deshane JS, Elmets CA, Athar M. Moving immune therapy forward targeting TME. *Physiol Rev*. 2021;101(2):417-425. doi:10.1152/physrev.00008.2020
8. Huang-Hobbs E, Cheng YT, Ko Y, et al. Remote neuronal activity drives glioma progression through SEMA4F. *Nature*. 2023;619(7971):844-850. doi:10.1038/s41586-023-06267-2
9. Kim SM, Lim EJ, Yoo KC, et al. Glioblastoma-educated mesenchymal stem-like cells promote glioblastoma infiltration via extracellular matrix remodelling in the tumour microenvironment. *Clin Transl Med*. 2022;12(8):e997. doi:10.1002/ctm2.997
10. Hoogstrate Y, Draaisma K, Ghisai SA, et al. Transcriptome analysis reveals tumor microenvironment changes in glioblastoma. *Cancer Cell*. 2023;41(4):678-692.e7. doi:10.1016/j.ccell.2023.02.019
11. Ferrer VP, Moura Neto V, Mentlein R. Glioma infiltration and extracellular matrix: key players and modulators. *Glia*. 2018;66(8):1542-1565. doi:10.1002/glia.23309
12. Bellail AC, Hunter SB, Brat DJ, Tan C, Van Meir EG. Microregional extracellular matrix heterogeneity in brain modulates glioma cell invasion. *Int J Biochem Cell Biol*. 2004;36(6):1046-1069. doi:10.1016/j.biocel.2004.01.013
13. Enegd B, King JA, Stylli S, Paradiso L, Kaye AH, Novak U. Overexpression of hyaluronan synthase-2 reduces the tumorigenic potential of glioma cells lacking hyaluronidase activity. *Neurosurgery*. 2002;50(6):1311-1318. doi:10.1097/00006123-200206000-00023
14. Yoo KC, Suh Y, An Y, et al. Proinvasive extracellular matrix remodeling in tumor microenvironment in response to radiation. *Oncogene*. 2018;37(24):3317-3328. doi:10.1038/s41388-018-0199-y
15. Cui Y, Cole S, Pepper J, Otero JJ, Winter JO. Hyaluronic acid induces ROCK-dependent amoeboid migration in glioblastoma cells. *Biomater Sci*. 2020;8(17):4821-4831. doi:10.1039/d0bm00505c
16. Martinez-Ordonez A, Duran A, Ruiz-Martinez M, et al. Hyaluronan driven by epithelial aPKC deficiency remodels the microenvironment and creates a vulnerability in mesenchymal colorectal cancer. *Cancer Cell*. 2023;41(2):252-271.e9. doi:10.1016/j.ccell.2022.11.016
17. Chan AT, Karakas MF, Vakrou S, et al. Hyaluronic acid-serum hydrogels rapidly restore metabolism of encapsulated stem cells and promote engraftment. *Biomaterials*. 2015;73:1-11. doi:10.1016/j.biomaterials.2015.09.001
18. Yi Z, Wenwen L, Kun W, Jian S. Overexpression of histone deacetylase 11 suppresses basal-like breast cancer cell invasion and metastasis. *Nan Fang Yi Ke Da Xue Xue Bao*. 2019;39(7):751-759. doi:10.12122/j.issn.1673-4254.2019.07.01
19. Li J, Yan X, Liang C, et al. Comprehensive analysis of the differential expression and prognostic value of histone deacetylases in glioma. *Front Cell Dev Biol*. 2022;10:840759. doi:10.3389/fcell.2022.840759
20. Fan Y, Peng X, Wang Y, Li B, Zhao G. Comprehensive analysis of HDAC family identifies HDAC1 as a prognostic and immune infiltration indicator and HDAC1-related signature for prognosis in glioma. *Front Mol Biosci*. 2021;8:720020. doi:10.3389/fmolb.2021.720020
21. Vengoji R, Atri P, Macha MA, et al. Differential gene expression-based connectivity mapping identified novel drug candidate and improved temozolomide efficacy for glioblastoma. *J Exp Clin Cancer Res*. 2021;40(1):335. doi:10.1186/s13046-021-02135-x
22. Dali-Youcef N, Froelich S, Moussallieh FM, et al. Gene expression mapping of histone deacetylases and co-factors, and correlation with survival time and 1H-HRMAS metabolomic profile in human gliomas. *Sci Rep*. 2015;20:9087. doi:10.1038/srep09087
23. Li Y, Li ZX, Jin T, Wang ZY, Zhao P. Tau pathology promotes the reorganization of the extracellular matrix and inhibits the formation

of perineuronal nets by regulating the expression and the distribution of hyaluronic acid synthases. *J Alzheimers Dis*. 2017;57(2):395-409. doi:10.3233/JAD-160804
24. Simone R, Javad F, Emmett W, et al. MIR-NATs repress MAPT translation and aid proteostasis in neurodegeneration. *Nature*. 2021;594(7861):117-123. doi:10.1038/s41586-021-03556-6
25. Wang D, Li J, Cai F, et al. Overexpression of MAPT-AS1 is associated with better patient survival in breast cancer. *Biochem Cell Biol*. 2019;97(2):158-164. doi:10.1139/bcb-2018-0039
26. Han X, Sekino Y, Babasaki T, et al. Microtubule-associated protein tau (MAPT) is a promising independent prognostic marker and tumor suppressive protein in clear cell renal cell carcinoma. *Urol Oncol*. 2020;38(6):605.e9-605.e17. doi:10.1016/j.urolonc.2020.02.010
27. Chandrashekar DS, Bashel B, Balasubramanya SAH, et al. UALCAN: a portal for facilitating tumor subgroup gene expression and survival analyses. *Neoplasia*. 2017;19(8):649-658. doi:10.1016/j.neo.2017.05.002
28. von Mering C, Jensen LJ, Snel B, et al. STRING: known and predicted protein-protein associations, integrated and transferred across organisms. *Nucleic Acids Res*. 2005;33(Database issue):D433-D437. doi:10.1093/nar/gki005
29. Warde-Farley D, Donaldson SL, Comes O, et al. The GeneMANIA prediction server: biological network integration for gene prioritization and predicting gene function. *Nucleic Acids Res*. 2010;38(Web Server issue):W214-W220. doi:10.1093/nar/gkq537
30. Han Y, Wang Y, Dong X, et al. TISCH2: expanded datasets and new tools for single-cell transcriptome analyses of the tumor microenvironment. *Nucleic Acids Res*. 2023;51(D1):D1425-D1431. doi:10.1093/nar/gkac959
31. Ratliff M, Karimian-Jazi K, Hoffmann DC, et al. Individual glioblastoma cells harbor both proliferative and invasive capabilities during tumor progression. *Neuro Oncol*. 2023;25(12):2150-2162. doi:10.1093/neuonc/noad109
32. Mehić M, de Sa VK, Hebestreit S, Heldin CH, Heldin P. The deubiquitinating enzymes USP4 and USP17 target hyaluronan synthase 2 and differentially affect its function. *Oncogenesis*. 2017;6(6):e348. doi:10.1038/oncsis.2017.45
33. Chen TC, Chuang JY, Ko CY, et al. AR ubiquitination induced by the curcumin analog suppresses growth of temozolomide-resistant glioblastoma through disrupting GPX4-mediated redox homeostasis. *Redox Biol*. 2020;30:101413. doi:10.1016/j.redox.2019.101413
34. Schubert M, Klinger B, Klünemann M, et al. Perturbation-response genes reveal signaling footprints in cancer gene expression. *Nat Commun*. 2018;9(1):20. doi:10.1038/s41467-017-02391-6
35. Wang Y, Zheng L, Shang W, et al. Wnt/beta-catenin signaling confers ferroptosis resistance by targeting GPX4 in gastric cancer. *Cell Death Differ*. 2022;29(11):2190-2202. doi:10.1038/s41418-022-01008-w
36. Wang Y, Zhao G, Condello S, et al. Frizzled-7 identifies platinum-tolerant ovarian cancer cells susceptible to ferroptosis. *Cancer Res*. 2021;81(2):384-399. doi:10.1158/0008-5472.CAN-20-1488
37. Wang GX, Tu HC, Dong Y, et al. ΔNp63 inhibits oxidative stress-induced cell death, including ferroptosis, and cooperates with the BCL-2 family to promote Clonogenic survival. *Cell Rep*. 2017;21(10):2926-2939. doi:10.1016/j.celrep.2017.11.030
38. Uhlén M, Fagerberg L, Hallström BM, et al. Proteomics. Tissue-based map of the human proteome. *Science*. 2015;347(6220):1260419. doi:10.1126/science.1260419
39. Sandelin A, Alkema W, Engström P, Wasserman WW, Lenhard B. JASPAR: an open-access database for eukaryotic transcription factor binding profiles. *Nucleic Acids Res*. 2004;32(Database issue):D91-D94. doi:10.1093/nar/gkh012
40. Mei S, Qin Q, Wu Q, et al. Cistrome data browser: a data portal for ChIP-seq and chromatin accessibility data in human and mouse. *Nucleic Acids Res*. 2017;45(D1):D658-D662. doi:10.1093/nar/gkw983
41. Feng C, Song C, Liu Y, et al. KnockTF: a comprehensive human gene expression profile database with knockdown/knockout of transcription factors. *Nucleic Acids Res*. 2020;48(D1):D93-D100. doi:10.1093/nar/gkz881
42. Kolmykov S, Yevshin I, Kulyashov M, et al. GTRD: an integrated view of transcription regulation. *Nucleic Acids Res*. 2021;49(D1):D104-D111. doi:10.1093/nar/gkaa1057
43. Goenka A, Khan F, Verma B, et al. Tumor microenvironment signaling and therapeutics in cancer progression. *Cancer Commun (Lond)*. 2023;43(5):525-561. doi:10.1002/cac2.12416
44. DePalma TJ, Sivakumar H, Skardal A. Strategies for developing complex multi-component in vitro tumor models: highlights in glioblastoma. *Adv Drug Deliv Rev*. 2022;180:114067. doi:10.1016/j.addr.2021.114067
45. Caon I, Bartolini B, Parnigoni A, et al. Revisiting the hallmarks of cancer: the role of hyaluronan. *Semin Cancer Biol*. 2020;62:9-19. doi:10.1016/j.semcancer.2019.07.007
46. Dixon SJ, Lemberg KM, Lamprecht MR, et al. Ferroptosis: an iron-dependent form of nonapoptotic cell death. *Cell*. 2012;149(5):1060-1072. doi:10.1016/j.cell.2012.03.042
47. Barayeu U, Schilling D, Eid M, et al. Hydropersulfides inhibit lipid peroxidation and ferroptosis by scavenging radicals. *Nat Chem Biol*. 2023;19(1):28-37. doi:10.1038/s41589-022-01145-w
48. Bourguignon LY, Peyrollier K, Xia W, Gilad E. Hyaluronan-CD44 interaction activates stem cell marker Nanog, Stat-3-mediated MDR1 gene expression, and ankyrin-regulated multidrug efflux in breast and ovarian tumor cells. *J Biol Chem*. 2008;283(25):17635-17651. doi:10.1074/jbc.M800109200
49. Zoltan-Jones A, Huang L, Ghatak S, Toole BP. Elevated hyaluronan production induces mesenchymal and transformed properties in epithelial cells. *J Biol Chem*. 2003;278(46):45801-45810. doi:10.1074/jbc.M308168200
50. Karousou E, Misra S, Ghatak S, et al. Roles and targeting of the HAS/hyaluronan/CD44 molecular system in cancer. *Matrix Biol*. 2017;59:3-22. doi:10.1016/j.matbio.2016.10.001
51. Chanmee T, Ontong P, Itano N. Hyaluronan: a modulator of the tumor microenvironment. *Cancer Lett*. 2016;375(1):20-30. doi:10.1016/j.canlet.2016.02.031
52. Porsch H, Bernert B, Mehić M, Theocharis AD, Heldin CH, Heldin P. Efficient TGFβ-induced epithelial-mesenchymal transition depends on hyaluronan synthase HAS2. *Oncogene*. 2013;32(37):4355-4365. doi:10.1038/onc.2012.475
53. Peng L, Fu J, Chen Y, et al. Transcription factor SNAI2 exerts protumorigenic effects on glioma stem cells via PHLPP2-mediated Akt pathway. *Cell Death Dis*. 2022;13(6):516. doi:10.1038/s41419-021-04481-2
54. Jin Y, Chen L, Li L, Huang G, Huang H, Tang C. SNAI2 promotes the development of ovarian cancer through regulating ferroptosis. *Bioengineered*. 2022;13(3):6451-6463. doi:10.1080/21655979.2021.2024319

SUPPORTING INFORMATION

Additional supporting information can be found online in the Supporting Information section at the end of this article.

How to cite this article: Liu Z, Yu K, Chen K, Liu J, Dai K, Zhao P. *HAS2* facilitates glioma cell malignancy and suppresses ferroptosis in an *FZD7*-dependent manner. *Cancer Sci*. 2024;115:2602-2616. doi:10.1111/cas.16232